Supporting Information

Self-doping memristors with equivalently synaptic ion dynamics for neuromorphic computing

Yaoyuan Wang, [†, §] *Ziyang Zhang,* [†, §] *Mingkun Xu,* [†, §] *Yifei Yang,* [†] *Mingyuan Ma,* [‡] *Huanglong Li,* [†] *Jing Pei* [†] *and Luping Shi*,* [†]

[†]Department of Precision Instrument, Center for Brain Inspired Computing Research, Beijing Innovation Center for Future Chip, [‡]Department of Electronic Engineering, Tsinghua University, Beijing, China, 100084

*E-mail: lpshi@mail.tsinghua.edu.cn

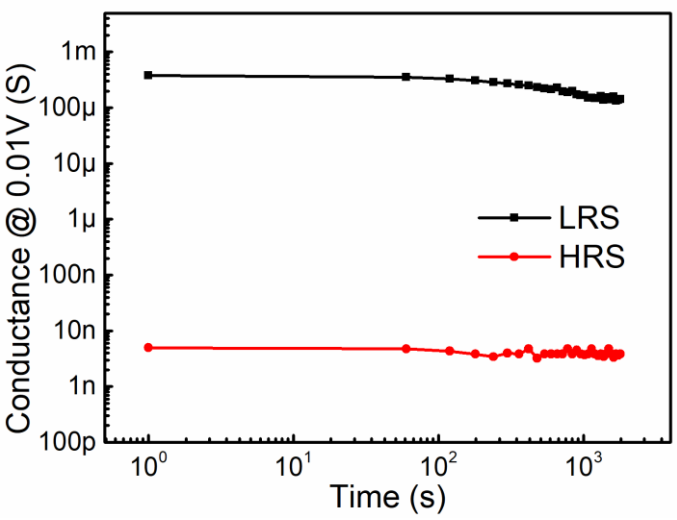

Figure S1 Nonvolatile properties of the device. The low resistance state (LRS) was measured after a positive voltage sweep from 0 to 0.6 V then back to 0 V, and the compliance current (CC) was 1 mA. The high resistance state (HRS) was measured after a negative voltage sweep from 0 to -0.6 V then back to 0 V.

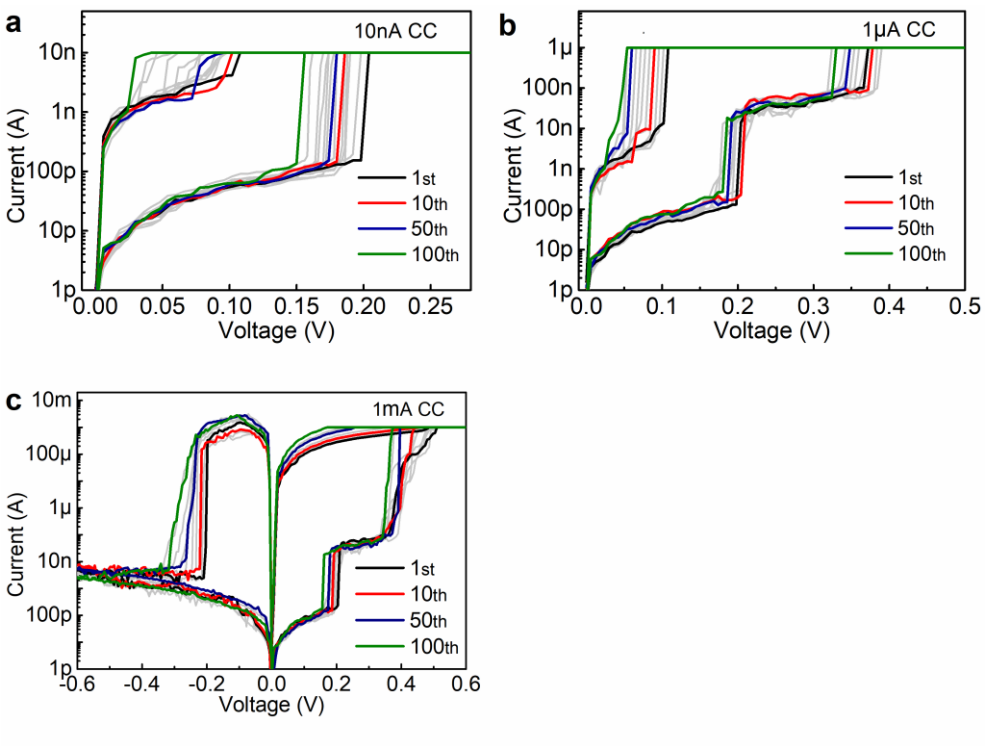

Figure S2 Endurance characteristics of the self-doping device. The CCs during positive sweeps are 10 nA (a), 1 μA (b) and 1 mA (c), respectively.

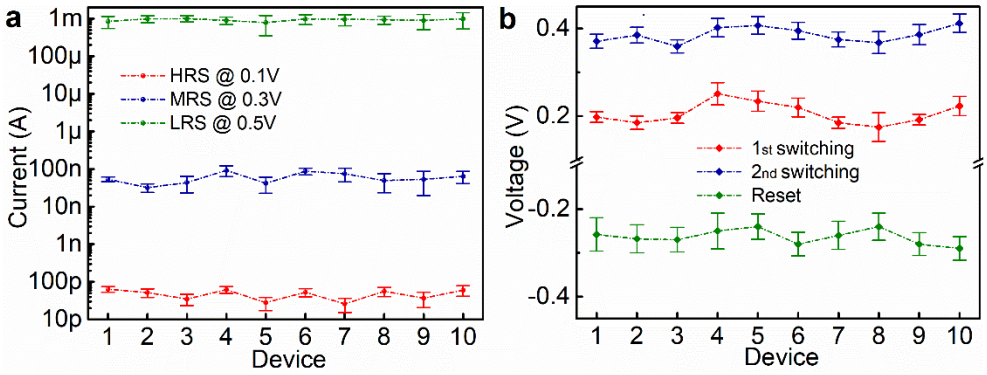

Figure S3 (a) Device-to-device variability of current levels at the LRS, the middle resistance state (MRS) and HRS. (b) Device-to-device variability of threshold voltages of the first switching, the second switching and the reset. The amplitude of each data is the average of 100 cycles measurement and the error bar is the standard deviation of them.

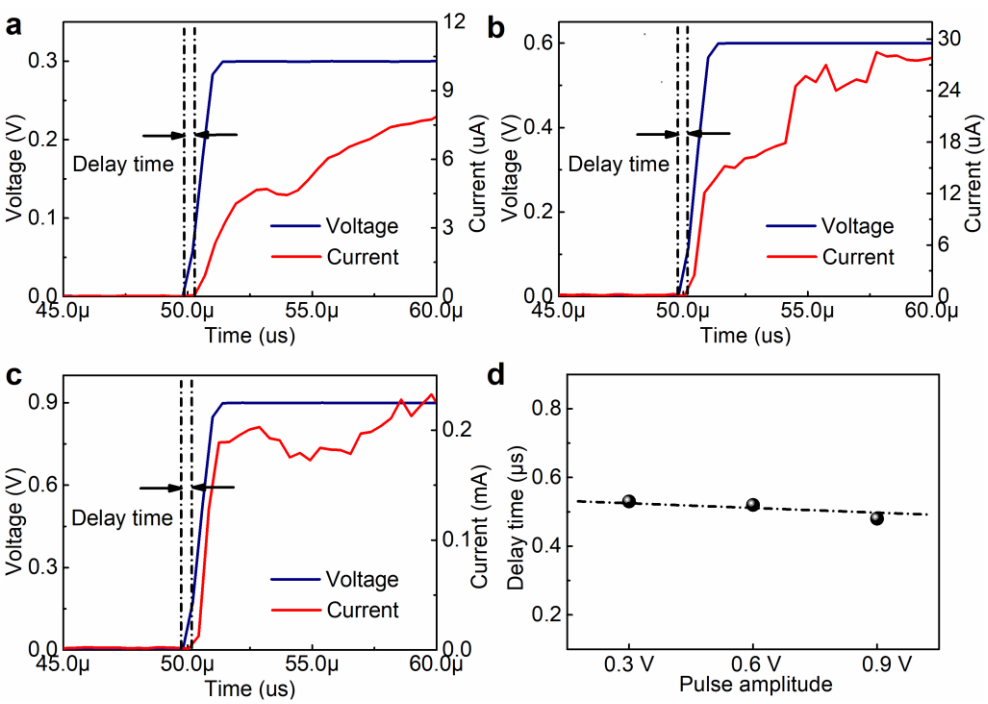

Figure S4 The delay time of the device under pulse amplitudes of (a) 0.3 V, (b) 0.6 V, (c) 0.9 V. (d) The delay time as a function of pulse amplitudes. We can see the threshold switching is slightly faster under a higher amplitude.

As shown in **Figure S5**a, an Ag/Ag:Ta_2O_5/Ag self-doping device was fabricated. A double switching behavior occurred during the positive sweep (Figure S1b). The first switching event was at 0.25V and another was at 0.45 V. During the negative sweep, however, only one switching event occurred. The threshold switching voltage was -0.4 V, which was approximate to the second threshold switching voltage in the positive side. These results indicated that the self-doping Ag atoms from the Ag bottom electrode played an important role in the double switching behavior. As shown in Figure S1c, we replaced the Ag top electrode with a Pt electrode in the artificial Ag doping device (Figure 2f in the main text). Only one switching event occurred in the negative switching at -0.25 V (Figure S1d). Compared with Figure 2g in the main text, a similar switching event occurred in ~ -0.2 V. Through these results, we can conclude that the first switching was determined by the artificial Ag doping layer.

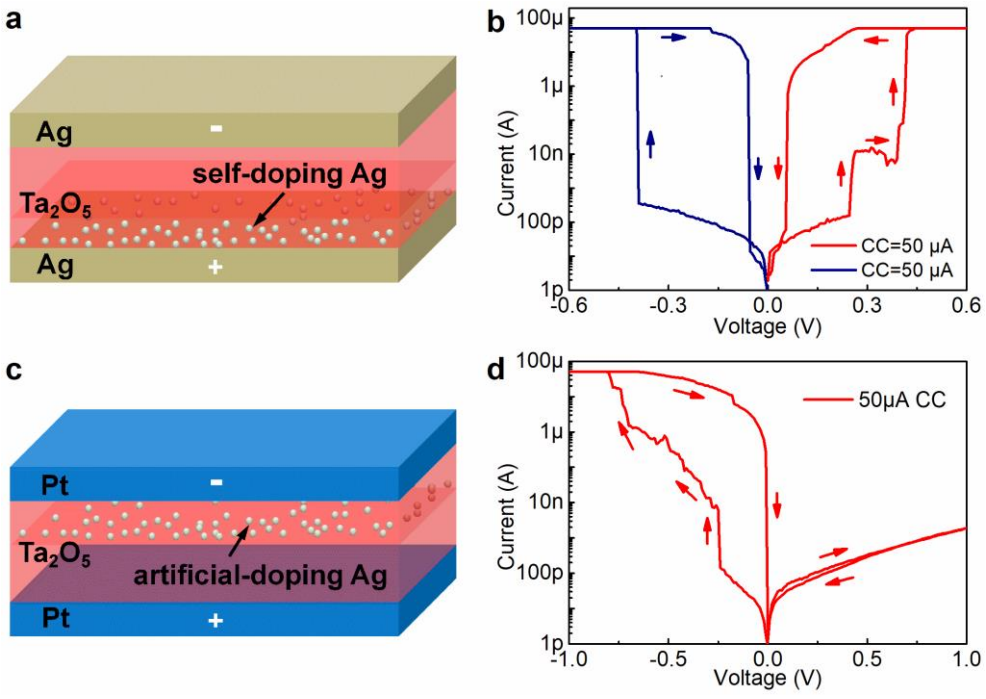

Figure S5 (a, c) Schematic diagram showing the cross section view of the Ag/Ag:Ta_2O_5/Ag self-doping device structure and Pt/Ta_2O_5/Ag:TaO_x/Pt artificial Ag doping device structure. (b) (d) Current-voltage (*I-V*) characteristics of the Ag/Ag:Ta_2O_5/Ag self-doping device and the Pt/Ta_2O_5/Ag:TaO_x/Pt artificial Ag doping device. During the measurement, the voltage was applied to the bottom electrode, whereas the top electrode grounded.

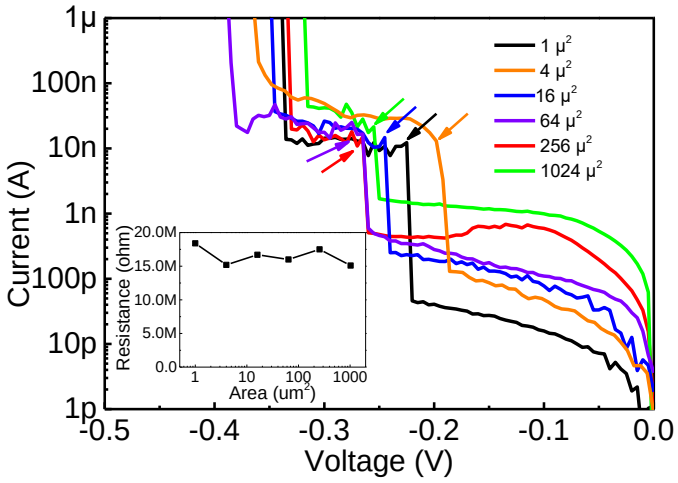

Figure S6 *I-V* characteristics of the self-doping memristors with different size. The inset shows the resistance at the switching point of each size, which is pointed out by the arrows.

As shown in **Figure S7**a, in the absence of the external stimuli, the neurotransmitters in the cleft recover back to the pre-synaptic terminal and the extrusion processes of Ca^{2+} occurs at the same time. In self-doping memristors, as shown in Figure S3b, as removing the external stimulus, the Ag atoms spontaneously diffuse and the weak Ag conductive filament spontaneously ruptures, which is similar to the synapses.

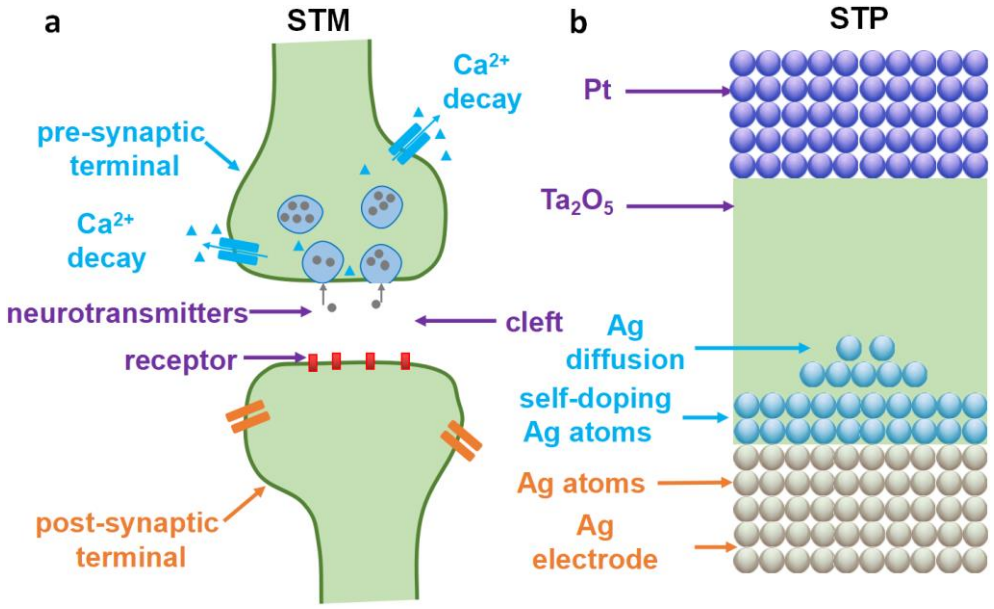

Figure S7 (a) The dynamic processes of Ca^{2+} decay and neurotransmitters replenishment after the elapse of the stimuli during the short-term memory. (b) The dynamic process of self-doping Ag atoms diffusion and the rupture of the conductive filament during the short-term plasticity of the memristor.

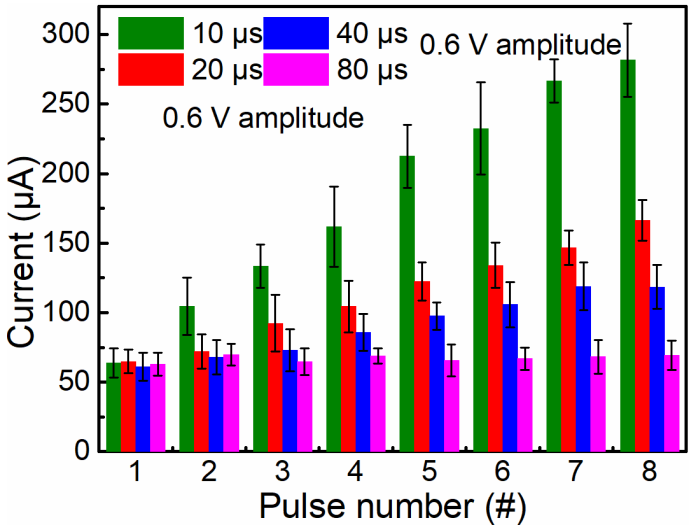

Figure S8 Average current through the memristor recorded after each pulse at different pulse intervals. The amplitude of each data is the average of ten devices measurement and the error bar is the standard deviation of them.

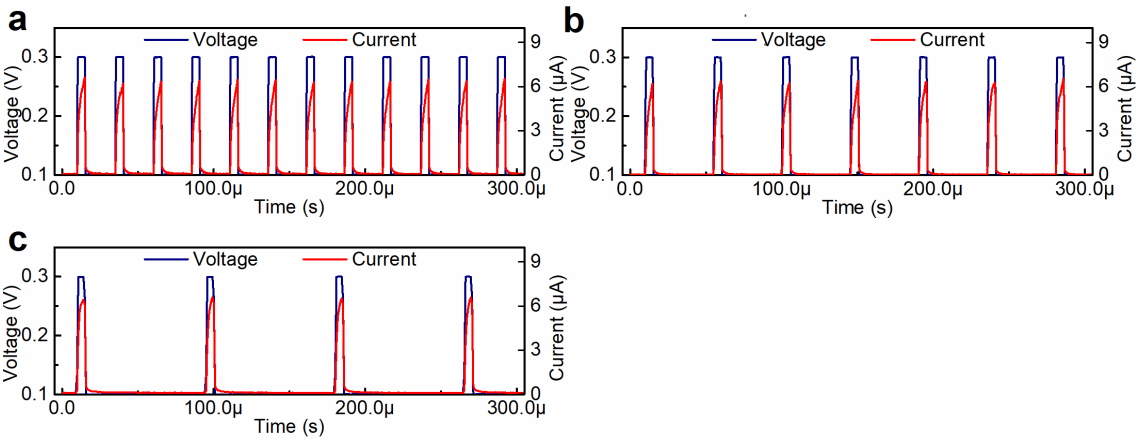

Figure S9 The current response of the device under continuous stimulating pulse with (a) 20 μs interval, (b) 40 μs interval, (c) 80 μs interval. The amplitude of the stimulating pulse is 0.3V and the width is 10 μs.

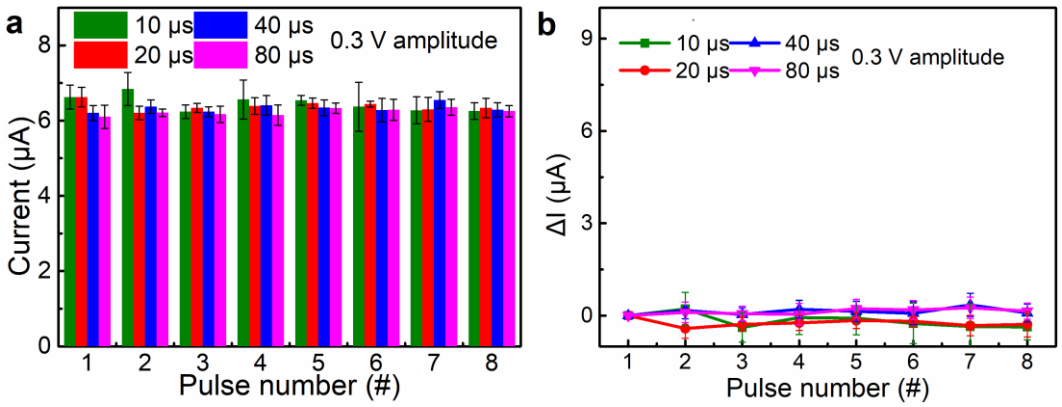

Figure S10 (a) Average current through the memristor recorded after each pulse at different pulse intervals. (b) Average current increase (ΔI) after each pulse at different pulse intervals. Here, ΔI is calculated by offsetting the current of each pulse with respect to the first pulse. The amplitude of each data is the average of ten devices measurement and the error bar is the standard deviation of them.

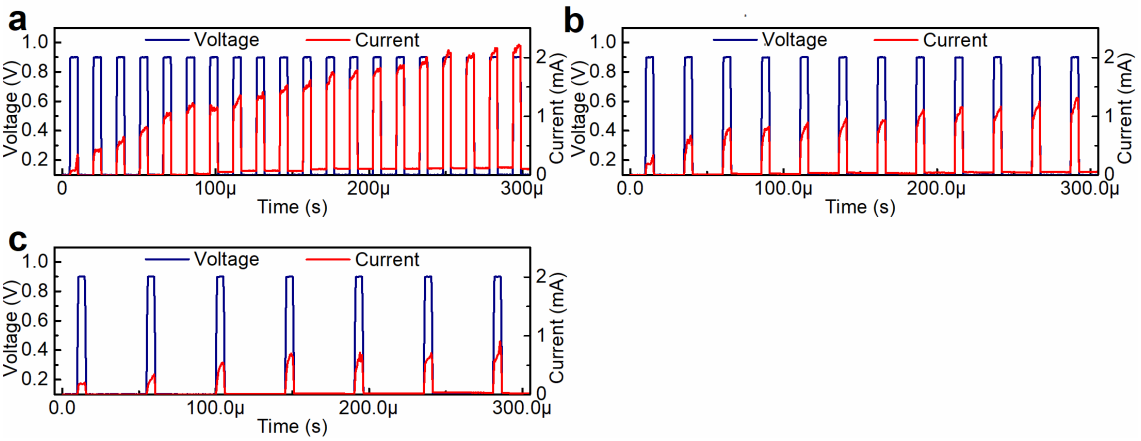

Figure S11 The current response of the device under continuous stimulating pulse with (a) 10 μs interval, (b) 20 μs interval, (c) 40 μs interval and (d) 80 μs interval. The amplitude of the stimulating pulse is 0.9V and the width is 10 μs.

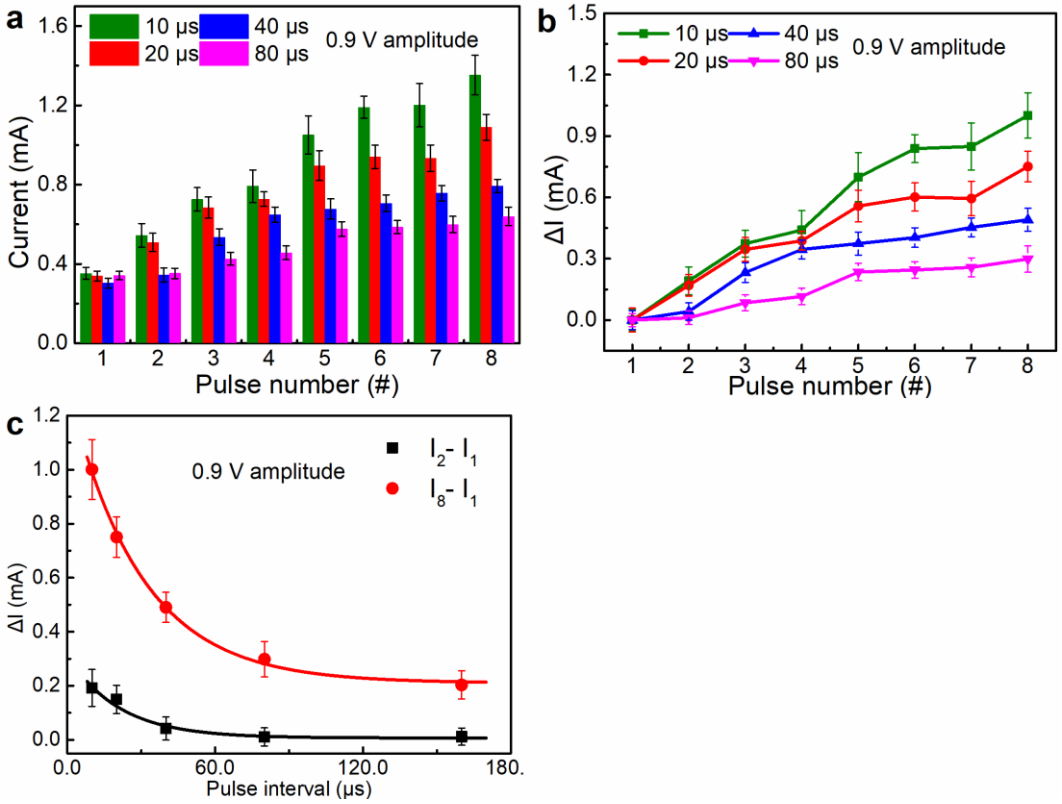

Figure S12 (a) Average current through the memristor recorded after each pulse at different pulse intervals. (b) Average Δ*I* after each pulse at different pulse intervals. Here, Δ*I* is calculated by offsetting the current of each pulse with respect to the first pulse. (c) Average Δ*I* after

consecutive pulses (I_2 - I_1) and after the eighth pulse (I_8 - I_1), which indicate PPF and PTP, respectively. The lines are fitted by an exponential function. The amplitude of each data is the average of ten devices measurement and the error bar is the standard deviation of them.

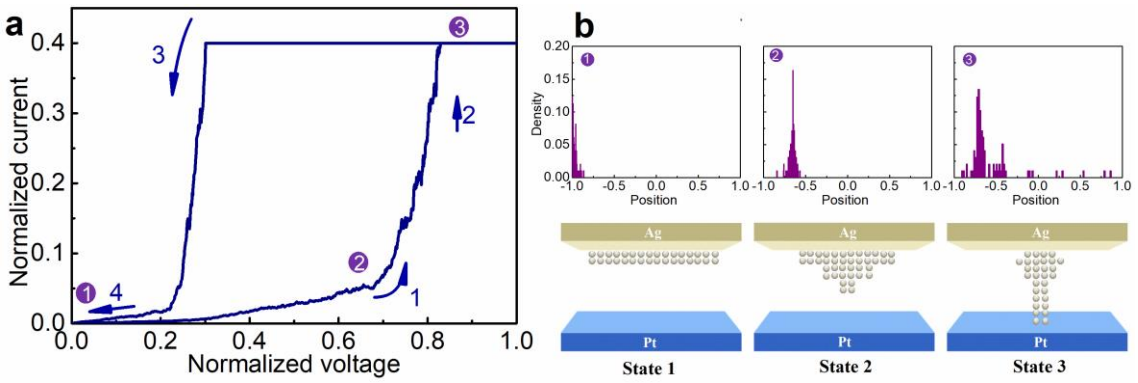

Figure S13 (a) Simulated *I-V* characteristic of normal Pt/Ta_2O_5/Ag memristor with single switching behavior. The normalized CC of the voltage sweep is 0.4. (b) Simulation results for the Ag nanoparticle density at selected instants during the voltage sweep, corresponding to the points labelled in (a). The inset figures below show schematic diagrams of the Ag nanoparticle positions.

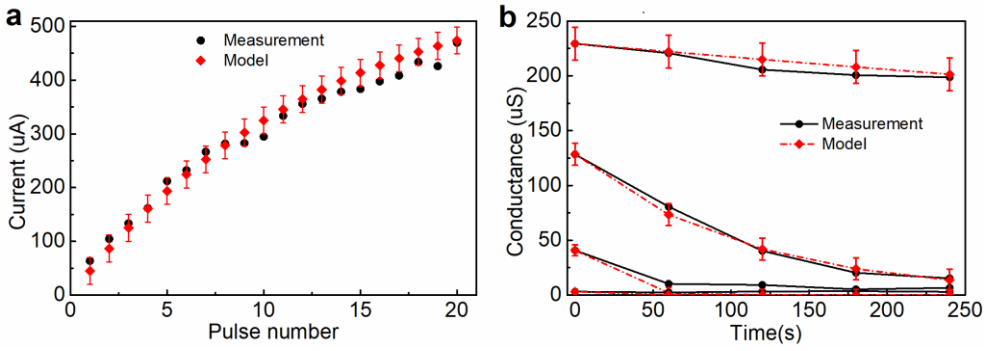

Figure S14 (a) Fitting results of the current response of the device under stimulus with 0.6 V amplitude and 10 μs intervals. (b) Fitting results of the conductance decay behavior.

Note S1 The description of exponential function in the conductance fitting of self-doping memristor.

The electrical conductivity of our device is given by the Arrhenius equation:[1-3]

$$R = R_0 \exp[\frac{E_{AC}}{k_B T}] \quad (1)$$

where T is the temperature of the device, R_0 is a pre-exponential factor which can be regarded as the extrapolated resistance at infinite T, k_B is the Boltzmann constant and E_{AC} is the activation energy for conduction. In this model, we assume that the R_0 linearly decreases with increasing conductive nanoparticle density (n_D), and the E_{AC} linearly decreases with increasing n_D. This relationship is also fund in the previous studies.[2-3] As shown in Figure 2a in the main text, we also assume that the average n_D of the device decreases linearly with the increasing sickness of the Ta_2O_5 layer.

$$R_0 = k_1 n_D + c_1 \quad (2)$$

$$E_{AC} = k_2 n_D + c_2 \quad (3)$$

$$n_D = k_3 L + c_3 \quad (4)$$

A simplified exponential formula from equation (1 ~ 4) is achieved to describe the conductance of the device:

$$R = (aL + b)exp(dL + e) \quad (5)$$

where

$$a = k_1 k_3 \quad (6)$$

$$b = k_1 c_3 + c_1 \quad (7)$$

$$d = \frac{k_2 k_3}{kT} \quad (8)$$

$$e = \frac{k_2 c_3 + c_2}{kT} \tag{9}$$

This function was used to fit the data in Figure 2b in the main text, and the result of the fitting equation is:

$$R = (0.11L + 0.21)\exp(0.81L - 0.18) \tag{10}$$

Note S2 The description of nanoparticle simulations of the device.

The nanoparticle simulations of the device are based on the Langevin equation.[4-6] In this model, we ignore the mass of the Ag nanoparticles, thus their diffusion can be described by an over-damped Langevin equation:

$$\alpha \frac{V(t)}{L} + \xi_i \sqrt{2\eta k_B T} - \frac{\partial U(x_i)}{\partial x_i} - \eta \frac{dx_i}{dt} = 0 \tag{11}$$

In the presence of the applied voltage $V(t)$, the Ag atoms are oxidized to Ag^+, a charge α is induced on the Ag nanoparticles, thus an electric force makes them move to the direction of electric field. The L is the thickness of the device between two electrodes. A random force with a white noise ξ_i is always on the Ag nanoparticles, its amplitude is influenced by the temperature T of the device. The k_B is the Boltzmann constant and the η is the nanoparticles viscosity. The U is the potential energy and has two energy scales, the interfacial energy U_I is responsible for the formation of large nanoparticles cluster near the electrode, and U_p is a weaker pinning energy with many smaller wells between two electrodes.

$$U = U_I + U_P = -w_I \left[exp\left(-\frac{(x_i + x_0)^2}{R_I^2}\right) + exp\left(-\frac{(x_i - x_N)^2}{R_I^2}\right)\right] + \frac{w_p}{2} sin\left(2\pi \frac{x}{R_P}\right) \tag{12}$$

Where w_I is the interfacial energy barrier, w_p is the amplitude of the pinning potential, x_0 and $-x_N$ are the positions of two electrodes, x_i is the position of Ag nanoparticles which are

normalized to [-1, 1], where x = -1 and 1 represent the position of bottom electrode and top electrode, respectively. The R_I and the R_P are the constant coefficients of U_I and U_P.

The temperature dynamics are described by Newton's law of cooling:

$$\frac{dT}{dt} = C_T \frac{V^2}{R} - \kappa(T - T_0) \tag{13}$$

where R is the device resistance, κ is the heat transfer coefficient, C_T is the heat capacitance and the T_0 is the background temperature.

The total resistance of the memristor is the sum of tunnelling resistances between N-1 adjacent Ag nanoparticles:

$$R = \sum_{i=0}^{N-1} \left(R_t e^{\frac{x_{i+1} - x_i}{\lambda}} \right) \tag{14}$$

where λ is the effective tunnelling length, R_t is the tunnelling resistance amplitude which is assumed same for all Ag nanoparticles.

The voltage, current and time in the simulation results are all dimensionless parameters. The time in the simulations is normalized by the temperature relaxation time 1/κ. The current in the simulations results is normalized by the maximal current that the memristor can reach. The voltage in the simulations results is normalized by the voltage that is a little bigger than the maximal threshold switching voltage.

Note S3 The description of short-term plasticity (STP) to long-term plasticity (LTP) transition model of the device in the neural network simulation.

A simplified dynamic model of the device was introduced to build the neural network.[7] To describe the STP to LTP transition of the device, we use a time parameter τ to represent the

facilitating efficiency of the device in response to the pulse stimuli. The τ is determined by the current conductance of the device:

$$\tau = aG(t)^b \tag{15}$$

where *G* is the conductance of the device, *a* and *b* are constants. After any given interval time Δt from the last spike at time *t*, the conductance of the device after spontaneous decay is:

$$G_{decay} = G(t)exp\left(\frac{-\Delta t}{\tau}\right) \tag{16}$$

This is an exponential decay that is determined by the interval time and time parameter τ. Finally, the conductance of the device is the sum of the conductance after decay and of a conductance increase by a programming spike if any is applied:

$$G(t+\Delta t) = \begin{cases} G_{decay} + U\left(A - G_{decay}\right) & \text{with spike} \\ G_{decay} & \text{no spike} \end{cases} \tag{17}$$

where *U* is the synaptic efficiency, *A* is the typical value extracted from device measurement.

The result of the fitting equation is: *A*=1000 μS, *U*=0.075, *a*=5E-9 s/μS^{-b}, *b*=4.9, for 0.6 V amplitude and 10 μs interval stimulus. We assume that the variability of the device is a Gaussian distribution with a constant deviation (25 μS) during the pulse stimuli, and we clip the negative or zero value. During the decay process (no spike), we assume that the standard deviation of the Gaussian distribution is related to the initial value, the constant scale factor is 0.8. The simulation results are shown in Figure S14.

REFERENCES

(1) Ielmini, D.; Nardi, F.; Cagli, C. Physical models of size-dependent nanofilament formation and rupture in NiO resistive switching memories. *Nanotechnology* **2011**, *22*, 254022.

(2) Larentis, S.; Nardi, F.; Balatti, S.; Gilmer, D. C.; Ielmini, D. Resistive Switching by Voltage-Driven Ion Migration in Bipolar RRAM—Part II: Modeling. *IEEE Trans. Electron Devices* **2012**, *59*, 2468-2475.

(3) Kim, S.; Choi, S. H.; Lu, W. Comprehensive Physical Model of Dynamic Resistive Switching in an Oxide Memristor. *ACS nano* **2014**, *8*, 2369-2376.

(4) Wang, Z.; Joshi, S.; Savel'ev, S. E.; Jiang, H.; Midya, R.; Lin, P.; Hu, M.; Ge, N.; Strachan, J. P.; et al. Memristors with diffusive dynamics as synaptic emulators for neuromorphic computing. *Nat. Mater.* **2017**, *16*, 101-108.

(5) Zhang, Z.; Wang, Y.; Li, H.; Wu, Y.; Wang, G.; Shi, L. Engineering the Synaptic Kinetic Process into Memristive Device. *Adv. Electron. Mater.* **2018**, *4*, 1800096.

(6) Wang, Y.; Zhang, Z.; Li, H.; Shi, L. Realizing Bidirectional Threshold Switching in Ag/Ta2O5/Pt Diffusive Devices for Selector Applications. *J. Electron. Mater.*, **2019**, *48*, 517-525.

(7) Barbera, S. L.; Vuillaume, D.; Alibart, F. Filamentary switching: synaptic plasticity through device volatility. *ACS nano* **2015**, *9*, 941-9.